Table 3. *Hydrogen atom positions in* $Cu(NO_3)_2.2{\cdot}5\ H_2O$

	PMR			DMR			X-ray		
	x	*y*	*z*	*x*	*y*	*z*	*x*	*y*	*z*
H(1)	0·270	0·118	0·124	0·269	0·124	0·123	0·267	0·11	0·120
H(2)	0·269	−0·191	0·100	0·270	−0·187	0·102	0·265	−0·18	0·099
H(3)	−0·033	0·079	0·088	−0·026	0·054	0·089	−0·025	0·05	0·091
H(4)	−0·016	0·209	0·175	−0·002	0·203	0·174	0·000	0·20	0·175
H(5)	0·423	−0·084	0·248	0·453	−0·079	0·245	0·452	−0·05	0·247

(*c*) *Hydrogen atom positions*

We have determined the hydrogen atom positions in $Cu(NO_3)_2.2{\cdot}5H_2O$ from the proton–proton vectors determined from the PMR study making use of the hydrogen-bonding scheme in the crystal (Morosin, 1970) and a method due to El Saffar (1966). We have also determined these positions from the orientation of the principal axes of the electric field gradient tensor found from DMR using a method outlined elsewhere (Vizia, Murty, Murty & Nagarajan, 1976). The hydrogen positions determined from PMR and DMR are shown in Table 3 along with those given by X-rays (Morosin, 1970). The agreement can be considered as satisfactory. Neutron diffraction is the technique used to determine accurately the hydrogen atom positions. To our knowledge, for $Cu(NO_3)_2.2{\cdot}5H_2O$ such a determination of the hydrogen positions has not been made. Hydrogen positions from X-ray studies are relatively less accurate and are not often determined. Positions found from the NMR study, while less accurate compared to those from a neutron diffraction study, are of value, particularly in the absence of the latter in the solution of the magnetic structure of antiferromagnetic crystalline hydrates. A larger number of hydrates appear to have been studied with NMR than with neutron diffraction.

The experiments were done on the Varian spectrometer at Tata Institute of Fundamental Research, Bombay. We thank Professor R. Vijaya Raghavan for his kind interest in this work. We also thank Dr G. Satyanandam for helpful discussions. The financial assistance by the CSIR and NSF (USA, GF 36748) is gratefully acknowledged.

References

DORNBERGER-SCHIFF, K. & LECIEJEWICZ, J. (1958). *Acta Cryst.* **11**, 825–827.
EL SAFFAR, Z. M. (1966). *J. Chem. Phys.* **45**, 4643–4651.
MOROSIN, B. (1970). *Acta Cryst.* B**26**, 1203–1205.
SODA, G. & CHIBA, T. (1969). *J. Chem. Phys.* **50**, 439–455.
VAN TOLL, M. W., HENKENS, L. S. J. M. & POULIS, N. J. (1971). *Phys. Rev. Lett.* **27**, 739–741.
VIZIA, N. C., MURTY, P. N., MURTY, C. R. K. & NAGARAJAN, V. (1976). *J. Magn. Reson.* **22**, 439–446.
VOLKOFF, G. M., PETCH, H. E. & SMELLIE, D. W. L. (1952). *Can. J. Phys.* **31**, 270–289.

Acta Cryst. (1982). A**38**, 304–310

On the Effect of Thermal Expansion on the Intensity of Diffraction from Molecules

BY D. YA. TSVANKIN

Institute of Elemento-Organic Chemistry of the USSR Academy of Sciences, 117813, *GSP*-1, *V*-334, *Vavilov st.* 28, *Moscow, USSR*

(*Received* 26 *March* 1981; *accepted* 24 *November* 1981)

Abstract

A number of polymers have been discovered recently for which the intensity of some Bragg reflections with $d >$ 10 Å considerably increases with temperature. Thermal expansion may be the reason for this anomalous phenomena. In sufficiently large molecules electron density distribution should change at the molecular boundaries upon thermal expansion. In the middle part of a molecule, owing to the rigidity of interatomic bonds, an increase in temperature will not cause appreciable changes. As a result, thermal expansion may lead to a re-distribution of the electron density and an increase in the intensity of Bragg reflections with temperature. The scattering from model systems of particles was calculated. The calculations show that the rate of the growth of the Bragg reflection intensity with maximum d increases when a relative size of the central part of particle with constant density increases. The larger the molecule, the faster the Bragg reflection intensity increases with temperature rise. Thermal expansion should lead to an increase in the intensity of

0567-7394/82/030304-07$01.00

Bragg reflections with largest d and thermal expansion should not affect the intensity of Bragg reflections at all if d values are small. The temperature factor of the intensity associated with thermal expansion should not depend on the Debye–Waller factor. The Debye–Waller factor characterizes the effect of thermal vibrations on the intensity of Bragg reflections in the harmonic approximation, while thermal expansion is related to anharmonic effects.

Introduction

Temperature changes in the intensity of diffraction peaks for all types of crystals are described by the Debye–Waller factor (Amoros & Amoros, 1968; Willis & Pryor, 1975). As the temperature increases, the amplitudes of atomic vibrations rise and, according to the Debye–Waller factor, the intensities of Bragg reflections have to decrease. The decrease in the intensity with temperature is typical of all Bragg reflections regardless of their Miller indices. The effect of thermal vibrations on the intensity of Bragg scattering is weakened with the increasing interplanar spacing d. If $d > 10$ Å, the Debye–Waller factor can change the intensity of Bragg reflection by no more than several per cent when the temperature is raised by several hundred degrees. Thus, the intensities of the Bragg reflections with large interplanar spacing should not actually depend on temperature if only the Debye–Waller factor is taken into account.

A number of substances have been found recently which appear to show a significant increase in the intensity of some Bragg reflections with increasing temperature. The reversible increase in the intensity of Bragg reflections was found for reflections with $d > 10$ Å in polymers with large molecules. This was observed with both crystalline substances (Matsushima & Hikichi, 1978) and mesomorphic structures (Tsvankin, Levin, Papkov, Zhukov, Zhdanov & Andrianov, 1979). In our previous work it was shown that the intensity and integral intensity of Bragg reflections increased reversibly in a number of polymers with mesomorphic structures. The intensity more than doubles as the temperature rises from 293 to 673 K. To explain this effect, the anomalous behaviour of the intensity of Bragg reflections was assumed to result from re-distribution of the average electron density in a molecule caused by thermal expansion (Tsvankin *et al.*, 1979). It is known that due to the high rigidity of interatomic bonds their length does not change noticeably with temperature, that is the thermal expansion reduces merely to the increase in intermolecular distances (Kitaigorodsky, 1973). The same situation takes place in polymeric crystals where the distances between macromolecules increase with the increasing temperature.

For a sufficiently large molecule the electron density distribution at its boundaries may change with the increasing temperature, while in the middle regions no appreciable changes can be expected because of the constancy of interatomic distances. Let us define the form factor of a molecule as a function characterizing the distribution of the intensity of scattering from the molecule considered as a body of a certain shape with constant electron density. The electron density vanishes in the transitional region at the body boundaries. Thermal expansion should cause an increase in the intermolecular distances and a change in the electron density distribution, *i.e.* a change in the form factor of a molecule or macromolecule. In the previous work calculations of scattering from a cylindrical model of a macromolecule were carried out in order to verify a scheme which describes the effect of thermal expansion on the intensity of Bragg reflections. The central region of the cylinder with a constant electron density was distinguished from the outer layer whose dimensions and density could vary, depending on temperature and thermal expansion. The calculations allowed us to obtain, for certain parameters of the model, the same increase in the intensity of reflections with increasing temperature, as in the experiment (Tsvankin *et al.*, 1979).

Explanation of the experimental data obtained leads to the problem concerning the temperature factor of the intensity of Bragg reflections. The Debye–Waller temperature factor cannot explain the considerable increase in the reflection intensities with the increasing temperature. It is necessary, therefore, to find an additional temperature factor of the intensity, proceeding from the effect of thermal expansion, that could explain these phenomena and must be common for both molecular and polymeric crystals.

In the present work diffraction from some of the simplest linear one-dimensional models is calculated. The calculations permit the estimation of the effect of parameters of the electron density distribution on the temperature changes in the molecular form factor and on the corresponding variation of the intensity of Bragg reflections. Proceeding from the calculations, the question is discussed, what should be the form of the temperature factor in order to account for the effect of thermal expansion on the intensity of various Bragg reflections.

The effect of thermal expansion on the intensity of diffraction from a linear system of particles

(*a*) *A linear system of particles with simple density distribution*

Let us consider first a linear system of particles with a relatively simple density distribution in the form of a

trapezoid. Assume all the particles to be identical with their lengths equal to $2L$ each. The particles are distributed along a straight line regularly with a period d (Fig. 1). Inside a particle, the central zone with a constant density $\delta = 1{\cdot}0$ has the length $2(l - \delta)$ (Fig. 2*a*). At the boundaries of each particle there are two transitional zones where the density decreases linearly from $\rho = 1{\cdot}0$ to 0, each zone having the length 2δ. The relationships between the parameters of the scheme in Fig. 2(*a*) are such that

$$L = l + \delta, \quad \delta < l < L, \quad l > 0{\cdot}5L. \tag{1}$$

Both the length of the particles and the distance between them increase, from $2L_1$ to $2L_2$ and from d_1 to d_2, respectively, with the increasing temperature (Figs. 1, 2). The drop in the electron density at the molecular boundaries should become less pronounced with the increasing amplitudes of thermal vibrations. The length of the boundary regions with variable density increases: $\delta_2 > \delta_1$, the length of the middle regions decreases: $l_2 - \delta_2 < l_1 - \delta_1$ since $l_2 = l_1$.

$$\frac{\delta_2}{L_2} > \frac{\delta_1}{L_1}; \quad \frac{l_2}{L_2} < \frac{l_1}{L_1}; \quad \frac{l_2}{L_2} - \frac{\delta_2}{L_2} < \frac{l_1}{L_1} - \frac{\delta_1}{L_1}. \tag{2}$$

Let us now calculate the form factor of the particle, F^2, and find how F and the intensity of Bragg reflection change on the variation of the electron density distribution due to thermal expansion (Fig. 2*b*). Let us denote the X-ray wavelength as λ and the scattering angle as 2θ. For the density distribution shown in Fig. 2(*a*), F may be calculated as follows:

$$F = \int_{-l-\delta}^{-l+\delta} \frac{x + l + \delta}{2\delta} \exp(isx)\,dx + \int_{-l+\delta}^{l-\delta} \exp(isx)\,dx + \int_{l-\delta}^{l+\delta} \frac{l + \delta - x}{2\delta} \exp(isx)\,dx.$$

$$F = \frac{2}{\delta s^2} \sin sl \sin s\delta = 2l \frac{\sin sl}{sl} \frac{\sin s\delta}{s\delta}, \tag{3}$$

$$s = \frac{4\pi \sin\theta}{\lambda}.$$

Let us consider first the intensity of the Bragg reflection corresponding to the period d in the arrangement of particles along the straight line of Fig. 1. In order to keep the analogy with the calculations of scattering from the system of cylindrical particles (Tsvankin *et al.*, 1979), we will assume that $d = 2{\cdot}1L$. In this case

$$sl = \frac{2\pi}{d} = 3{\cdot}0 \frac{l}{L}, \quad s\delta = 3{\cdot}0 \frac{\delta}{L}. \tag{4}$$

In order to find how F changes with the increasing L, let us consider F'_L as obtained from (3), (4),

$$F'_L = \frac{l(l - \delta)}{L} \left[\frac{\sin s(l - \delta)}{s(l - \delta)} - \frac{\sin sl}{sl} \frac{\sin s\delta}{s\delta} \right]. \tag{5}$$

It follows from the conditions (1), (2) and from the monotonic decrease of the function $\sin x/x$ in the interval $0 < x < \pi$ that for a reflection satisfying (4) the condition $F'_L > 0$ always holds. In other words, the temperature changes in the electron density distribution shown in Fig. 2(*b*) will always cause the growth of F and the increase in the reflection intensity.

Tables 1 and 2 present the results of a series of calculations which show the relationship between the electron density distribution in the particle, thermal expansion and the Bragg reflection intensity. The changes in the reflection intensity owing to thermal expansion are determined by the parameter $P = F_2^2/F_1^2$. F_1 and F_2 were calculated using (3), (4). F_1 refers to the particles before expansion with the length L_1 at the distance d_1 from one another. F_2 refers to the particles after expansion with the length L_2, distributed with the period d_2 (Figs. 1, 2). Besides F_1 and F_2, F_3 was also calculated by the same equations (3), (4) for particles with length L_1 and initial density distribution, which are placed not at a distance d_1 but at d_2 from one another. F_3^2 describes the reflection intensity for the case where the density distribution inside the particle remains constant and only the distances between the particles

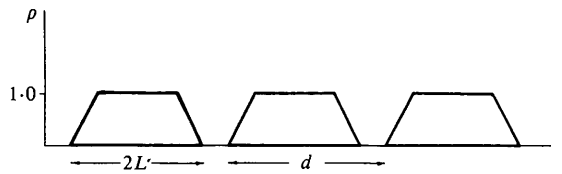

Fig. 1. Scheme of distribution of particles along a straight line. d = distance between particles, $2L$ = length of a particle.

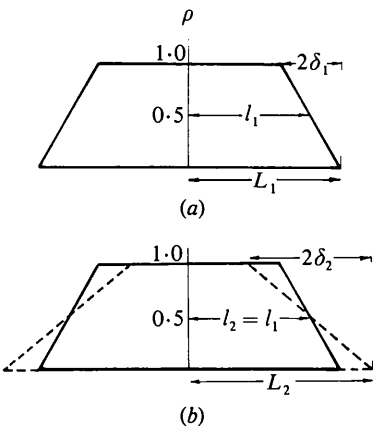

Fig. 2. (*a*) Electron density distribution in a particle before expansion. (*b*) Dotted line represents the electron density distribution after thermal expansion.

increase from d_1 to d_2 with the changing temperature (Fig. 1). Note that F_2^2 was also calculated for the lattice with the period d_2, though with the form factor changed due to thermal expansion. The parameter $P = F_2^2/F_1^2$ represents the total change in the reflection intensity owing both to the increasing distance between the particles and to the change in their form factor. On the other hand, the values of $Q = F_2^2/F_3^2$ also listed in Tables 1, 2 characterize the changes in the reflection intensity owing to the change in the form factor only, since F_2 and F_3 have been calculated for the same period d_2. Comparing P and Q one may distinguish between the effect of change in the form factor of particles on the reflection intensity and the effect of increasing distances between the particles.

The results of calculations of P and Q are given in Table 1 where the electron density distribution parameter l_1/L_1 varies, but the thermal expansion is the same: $L_2 = 1{\cdot}05L_1$ and $d_2 = 1{\cdot}05d_1$. The data of Table 2 were obtained for the constant value of the parameter $l_1/L_1 = 0{\cdot}8$, but for various thermal expansions $L_2 = kL_1$, $d_2 = kd_1$; where k ranges from 1·012 to 1·15.

It is seen from Tables 1, 2 that $P > 1$ for all cases. It follows from the results of Table 1 that the increase in the intensity is determined by the parameter l_1/L_1. The greater l_1/L_1 and the less the length of the transitional region $2\delta_1/L_1$, the more efficient is the increase in the reflection intensity. The value of P also increases proportionally to thermal expansion. As can be seen from Table 2, the increase in k at the constant value of l_1/L_1 leads to a considerable increase in P, *viz* from 1·06 to 1·88.

In Tables 1, 2 $Q \leq 1{\cdot}0$, *i.e.* the changes in the form factor of a particle do not increase, but decrease the intensity of the Bragg reflection in question. The intensity grows ($P > 1$, Tables 1, 2) in this case not because of changes in the form factor of the particle but owing to an increase in the distance between the particles. The result $Q < 1{\cdot}0$ means that the theoretical intensity of the Bragg reflections, as calculated neglecting the changes in the form factor of particle F_3^2, exceeds, at a given temperature T_2, the 'experimental' intensity that takes into account these changes: $F_2^2 < F_3^2$. In other words, with the above model (Figs. 2*a*,*b*) the effect of the thermal expansion factor Q is similar to the effect of the Debye–Waller temperature factor, which also causes a decrease in the Bragg reflection intensities.

Table 1. *Calculation of P and Q with constant thermal expansion and various electron density distribution parameters*

$k = 1{\cdot}05$.

l_1/L_1	δ_1/L_1	δ_2/L_2	F_1	P	Q
0·55	0·45	0·47	43·2	1·03	0·85
0·60	0·40	0·43	42·2	1·04	0·88
0·70	0·30	0·33	35·6	1·18	0·91
0·80	0·20	0·24	26·5	1·28	0·94
0·90	0·10	0·14	15·8	1·69	0·96
0·95	0·05	0·09	10.0	2·35	0·96
1·00	0·00	0·05	5·0	3·70	1·00

(b) A linear system of particles with more complicated electron density distribution

As another example, let us consider a particle with a more complicated electron density distribution (Fig. 3).

Unlike the previous case (Fig. 2), the boundary regions with length f_1 and constant density $\rho_1 < 1{\cdot}0$ were introduced in the density distribution in Fig. 3. Between the regions of constant density two transitional regions, both 2δ long, are located where the density decreases linearly from 1 to ρ_1. As a result of thermal expansion and increase in the length of the particle (from $2L_1$ to $2L_2$) the boundary regions change so that their density decreases, $\rho_2 < \rho_1$. The zones of transitional density become longer but the central region with $\rho = 1$ remains unchanged (Fig. 3). For the calculation of the form factor of a particle, F^2, the total density distribution in Fig. 3 may be imagined to consist of two parts. One of them has the length $2L_1$ and constant density ρ_1. The other part is analogous to the distribution discussed above (Fig. 2*a*), with the density $1 - \rho_1$. Since the total density distribution in Fig. 3 is the sum of these two parts, F may also be considered as the sum of two terms,

Table 2. *Calculation of P and Q with constant value of l_1/L_1 for various thermal expansions*

$l_1/L_1 = 0{\cdot}8$; $\delta_1/L_1 = 0{\cdot}20$.

k	δ_2/L_2	P	Q
1·012	0·21	1·06	0·98
1·025	0·22	1·14	0·96
1·05	0·24	1·28	0·94
1·075	0·25	1·49	0·92
1·10	0·27	1·65	0·88
1·125	0·29	1·77	0·85
1·15	0·30	1·88	0·82

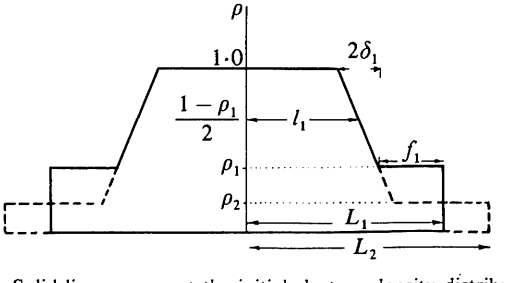

Fig. 3. Solid lines represent the initial electron density distribution before expansion. Dotted line shows the density distribution after thermal expansion.

$$F = 2L_1\rho_1\frac{\sin sL_1}{sL_1} + 2l_1(1-\rho_1)\frac{\sin sl_1}{sl_1}\frac{\sin s\delta_1}{s\delta_1}. \quad (6)$$

F_1 is determined from (6) using the values L_1, ρ_1, l_1 and δ_1 (Fig. 3). To calculate F_2 corresponding to the particle after expansion, it is necessary to know ρ_2, l_2, δ_2. These may be found by postulating the conservation of the 'electron mass' of the particle which is equal to the area under the density distribution curve (Fig. 3). Assuming the slope of the straight line in the transitional region to remain constant upon expansion, as in Fig. 3, we obtain:

$$\frac{1-\rho_1}{2\delta_1} = \frac{1-\rho_2}{2\delta_2} = c; \quad \varphi = L_2 - L_1$$
$$\varepsilon = f_1 + \varphi - [(f_1+\varphi)^2 - 2\rho_1\varphi/c]^{1/2} \quad (7)$$
$$l_2 = l_1 + 0{\cdot}5\,\varepsilon; \quad \rho_2 = \rho_1 - c\varepsilon.$$

Since δ_2 does not affect the 'electron mass' of the particle the values for δ_2 are chosen arbitrarily with the condition that $\delta_2 < l_2$ or $\delta_2 < L_1 - l_2$. The calculation of the derivative F'_L in its general form by (6), (7) is very complicated. The ratios $P = F_2^2/F_1^2$ and $Q = F_2^2/F_3^2$ for various values of the density distribution parameters were calculated by (6), (7) in order to describe the changes in the intensity of the Bragg reflection corresponding to the distance $d = 2{\cdot}1L$ between the particles (Table 3). As in the previous case, F_1 describes the particles of length L_1 before expansion, F_2 refers to particles of length L_2 and changed density distribution, the particles being located at distances d_2 from one another. F_3 was calculated for the particles of the initial density distribution with the length L_1 arranged along a straight line with the period d_2. The parameter P describes the overall change in the reflection intensity upon thermal expansion and Q, which is independent of the distance between the particles, represents only the effect of the particle form factor. As in the previous calculations, $L_2 = 1{\cdot}05L_1$. In Table 3, computations 1, 2, 3 were done for $\delta_1 = 0$ when there was no transitional density zone. Under these conditions, the higher ρ_1, the greater is the growth of the intensity. Note that for cylindrical particles with a similar scheme of electron density distribution the increase in ρ_1 also leads to a faster rise of the reflection intensity, as shown in the previous communication (Tsvankin *et al.*, 1979). The closer δ_2/L_2 is to δ_1/L_1, the faster the intensity rises and, *vice versa*, the greater the difference between δ_2/L_2 and δ_1/L_1, the smaller is the value of P. For instance, in computation 4 $P = 1{\cdot}19$ for δ_2/L_2, $\delta_1/L_1 = 0{\cdot}2$ and the intensity increases by 20%. At the same time, $P = 0{\cdot}85$ for $\delta_1/L_1 = 0{\cdot}2$ and $\delta_2/L_2 = 0{\cdot}4$ (computation 5), *i.e.* the reflection intensity no longer increases, but decreases during thermal expansion.

Table 3. *Calculations for P and Q*

	l_1/L_1	δ_1/L_1	δ_2/L_2	ρ_1	P	Q
1	0·5	0	0	0	1·08	1·0
2	0·5	0	0	0·3	1·16	0·96
3	0·5	0	0	0·7	1·39	0·84
4	0·5	0·20	0·202	0·3	1·19	0·97
5	0·5	0·20	0·40	0·3	0·85	0·69
6	0·5	0·30	0·38	0·3	1·41	1·16
7	0·5	0·30	0·43	0·3	1·21	0·96
8	0·7	0	0	0	1·25	1·0
9	0·7	0	0	0·7	1·74	0·92
10	0·7	0·10	0·11	0·3	1·39	1·02
11	0·7	0·10	0·30	0·3	1·08	0·79
12	0·7	0·20	0·22	0·3	1·46	1·04
13	0·85	0	0	0	1·55	1·0
14	0·85	00	0	0·7	2·53	1·02
15	0·85	0·10	0·12	0·3	1·67	1·17

As far as the parameter l_1/L_1 is concerned, its increase leads to a quite fast rise of P. This is clear from the comparison of computations 1, 8, 13 with 3, 9, 14 and 4, 12 which have been done for different l/L but equal or close values of δ_1/L_1 and ρ_1.

In a number of cases (6, 10, 12, 14, 15) Q turned out to be more than unity. In these variants the 'experimental' intensity must be higher than the theoretical one calculated for the same lattice neglecting thermal expansion ($Q > 1$, $F_2^2 > F_3^2$). Under these conditions, the temperature factor due to thermal expansion should lead, unlike the Debye–Waller factor, to an increase in the intensity of the Bragg reflection under consideration. For the rest values of the parameters, calculations based on a more complicated scheme (Fig. 3) lead, as before, to $Q \leq 1$.

In all the cases, except 14, in order to obtain $Q > 1$ one needs to suppose the existence of transitional zones $\delta_1/L_1 \neq 0$ as well as a sufficiently large value of P, *i.e.* insignificant difference between δ_2/L_2 and δ_1/L_1.

(c) *Intensity changes in other Bragg reflections*

Up to now we have analysed the temperature variation of the first, major Bragg reflection, associated with the regular location of particles (with the period $d = 2{\cdot}1L$) along a straight line (Fig. 1). To find

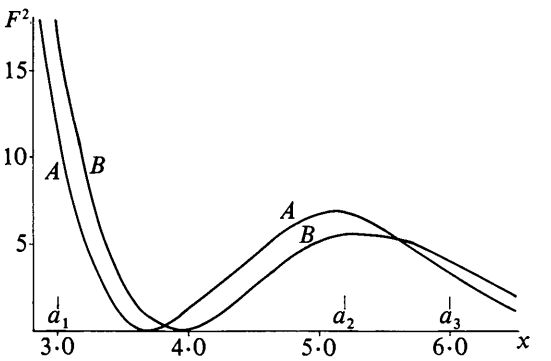

Fig. 4. Form factors of the particle (Fig. 3), as calculated by (6), (7), (8). (*A*) $F_1^2(x)$ – before expansion, (*B*) $F_2^2(x)$ – after expansion.

the changes in the intensity of other Bragg reflections, let us consider the entire curve $F^2(x)$ of the particle form factor ($x = sL = 2\pi L/d$). The entire curve $F^2(x)$ was calculated by the same equations (6), (7) that were used to obtain the data of Table 3. The following values of the parameters were chosen:

$$l_1/L_1 = 0{\cdot}7; \quad \delta_1/L_1 = 0{\cdot}1; \quad \rho_1 = 0{\cdot}5; \quad L_2 = 1{\cdot}05\,L_1. \tag{8}$$

The curves $F_1^2(x)$ and $F_2^2(x)$ thus obtained are given in Fig. 4. As before, F_1^2 characterizes the particle before expansion and F_2^2 is the form factor of the particle after expansion. It can be seen from Fig. 4 that $F_2^2 > F_1^2$ and $P > 1$ for $x < 3{\cdot}8$. Thus, if a Bragg reflection lies in this region ($x < 3{\cdot}8$), its intensity increases upon thermal expansion. In the next interval $3{\cdot}8 < x < 5{\cdot}6$ the curve F_1^2 goes higher than the F_2^2 curve and $P < 1$ (Fig. 4). The intensity of Bragg reflections from this interval will not increase but decrease on thermal expansion. For greater values $x > 6$ the curves F_1^2 and F_2^2 are close to each other and $P \simeq 1$. Let us assume the linear system to be a model of the planar hexagonal lattice. Then the subsequent Bragg reflections will be located at points $a_1 = 3{\cdot}0$, $a_2 = 1{\cdot}73a_1 = 5{\cdot}2$ and $a_3 = 2a_1 = 6{\cdot}0$. The values of a_1, a_2 and a_3 are given in Fig. 4. For these reflections $P_1 = 1{\cdot}53$, $P_2 = 0{\cdot}82$ and $P_3 = 1{\cdot}22$; that is the intensity of the first and third reflections must increase and the intensity of the second reflection must decrease with increasing temperature.

Discussion

The main purpose of the above calculations was to explain the experimentally observed increase in the intensity of Bragg reflections with the increasing temperature (Matsushima & Hikichi, 1978; Tsvankin *et al.*, 1979). The calculations of scattering were based on the natural assumption that for a sufficiently large molecule the electron density distribution changes, upon thermal expansion, only near its boundaries, but remains unchanged in the middle region of the molecule. To simulate such changes, two linear schemes of the arrangement of particles (molecules) were considered (Figs. 2, 3). The calculations based on these schemes show (Tables 1, 2, 3) that for most of the cases the intensity of Bragg reflections with maximum d should increase ($P > 1$), to some extent, upon thermal expansion, the increase being faster the greater the parameter l_1/L_1 is, that is, the larger the initial size of the middle region of constant density is. The latter circumstance, obviously, explains the fact that the growth of the intensity of Bragg reflections with temperature is observed for large molecules. Indeed, the size of the transitional region near the boundaries of a molecule should be approximately the same for different molecules, while the dimensions of the middle region of constant density increase proportionally to the size of the entire molecule. Therefore, the larger the molecule, the greater l_1/L_1 must be and the faster the intensity of the corresponding Bragg reflections should rise. Besides, only in crystals with sufficiently large molecules may one find the reflections with $d > 10$ Å which are slightly affected by the Debye–Waller factor. It should be recalled that the increase in the intensity is to be observed only for Bragg reflections with the largest d values, as can be seen from Fig. 4. For smaller d values the intensity may either decrease or remain constant, depending on the reflection position and on the magnitude of thermal expansion.

The quantities describing changes in the form factors of the particles Q are like a temperature factor of the reflection intensity which is caused by thermal expansion. The effect of thermal expansion on the intensity of Bragg reflections and, accordingly, the values of Q should be independent of the Debye–Waller factor which describes the effect of thermal vibrations on the intensity of Bragg reflections in the harmonic approximation. Thermal expansion and the related effects cannot be calculated in the harmonic approximation. Anharmonic corrections for the Debye–Waller factor were calculated and experimentally found for a number of crystals (Willis & Pryor, 1975). Perhaps, the factor Q associated with thermal expansion should be such an anharmonic correction for molecular and polymeric crystals.

In low-ordered mesomorphic structures the centres of molecules form a lattice, while single atoms are distributed in a random way. In this case the Debye–Waller factor, which is related to individual atoms, cannot be calculated at all. For mesomorphic structures the total intensity distribution is determined by the form factor of a molecule or macro-molecule and by its changes under thermal expansion. For molecular and polymeric structures with an ordinary crystal lattice the Q factor should probably be introduced as a correction multiplier to the Debye–Waller factor.

The form factor of a real molecule and, correspondingly, its Q value may be described if the molecule is represented as a continuous body of a definite shape with its boundaries determined by intermolecular radii. The electron density vanishes within the transitional zone at the boundaries of the molecule. A particular size of transitional zone should correspond to every temperature. This refers to fairly large molecules, in which central regions with a constant density can be distinguished. Electron density distributions in a molecule that correspond to a given temperature and to zero temperature can be constructed using the well-known formulae of X-ray diffraction analysis (Amoros & Amoros, 1968). Comparison of these distributions may permit the determination of the changes caused by thermal expansion. It is also possible to take a linear change in the density, at the boundary of a molecule (similar to Fig. 2*b*) as the first approximation.

References

AMOROS, J. L. & AMOROS, M. (1968). *Molecular Crystals: Their Transforms and Diffuse Scattering*. New York: Wiley.

KITAIGORODSKY, A. I. (1973). *Molecular Crystals and Molecules*. New York, London: Academic Press.

MATSUSHIMA, N. & HIKICHI, K. (1978). *Polym. J.* **10**, 437–441.

TSVANKIN, D. YA., LEVIN, V. JU., PAPKOV, V. S., ZHUKOV, V. P., ZHDANOV, A. A. & ANDRIANOV, K. A. (1979). *Vysokomol. Soedin. Ser. A*, **21**, 2126–2135.

WILLIS, B. T. M. & PRYOR, A. W. (1975). *Thermal Vibrations in Crystallography*. Cambridge Univ. Press.

Acta Cryst. (1982). A**38**, 310–317

High-Resolution Images of Ordered Alloys by High-Voltage Electron Microscopy

BY D. SHINDO

The Research Institute for Iron, Steel and Other Metals, Tohoku University, Sendai, Japan

(*Received* 10 *September* 1981; *accepted* 17 *November* 1981)

Abstract

The image formation of high-voltage, high-resolution electron microscopy of ordered alloys has been studied on the basis of many-beam dynamical diffraction theory. It is revealed that superstructure images are observable for a rather thick crystal when nearly kinematical relationships hold among certain beams of the superlattice reflections; these beams are almost in phase and have amplitudes proportional to their structure factors. Thickness dependences of the phase differences and the scattering amplitudes are calculated for the superstructure of $D0_{23}$ type of the gold-based alloys Au_3X (X = Mg, Zn and Cd). The results are discussed in connection with the difference in atomic scattering factors of the constituents X. The contrast of the superstructure image is discussed in terms of the amplitude–phase diagram of the superlattice reflections.

I. Introduction

The many-beam imaging technique has been developed for high-resolution electron microscopy to investigate structures of crystalline and amorphous materials (Iijima, 1971). Amelinckx and his colleagues have made extensive high-resolution studies on ordered alloys using 100 kV electron microscopes [Amelinckx, 1978–79; Van Tendeloo, 1980]. The many-beam imaging technique with the use of a 1 MV electron microscope has been applied to the study of superstructures of gold-based alloys with Cd, Mn and Mg (Hiraga, Hirabayashi & Shindo, 1977; Hiraga, Shindo, Hirabayashi, Terasaki & Watanabe, 1980; Terasaki, Watanabe, Hiraga, Shindo & Hirabayashi, 1980). In these observations, the solute atom positions projected along the incident beam appear as either bright or dark dots, and can be identified at the atomic level from comparison with the calculations based on dynamical diffraction theory. In this respect, high-voltage, high-resolution electron microscopy [HVHREM] is a powerful means for the investigation of ordered structures (Hirabayashi, 1980; Hirabayashi, Hiraga & Shindo, 1981).

High-resolution images which are interpretable in terms of ordered atomic arrangements are called superstructure images (Hiraga, Shindo & Hirabayashi, 1981). These images do not reflect a projection of crystal potential itself, which may be interpreted in the weak-phase-object approximation, but exhibit the atom columns of constituent B in A_3B alloys projected down along the incident beam. The superstructure images are contributed dominantly by superlattice reflections rather than fundamental reflections.

We have observed previously the superstructure images of Au–Cd alloys of several hundred ångströms thickness. In the successive experiments on such alloys as Au–Mg, Au–Mn and Au–Zn, however, we noticed that the superstructure images were not always observable for foils as thick as in the case of the Au–Cd alloy. It is worthwhile, therefore, to clarify the theoretical background for the formation of superstructure images of ordered alloys. In this paper, we first deal with the dynamical electron scattering from ordered alloys using the multislice formulation (Cowley & Moodie, 1957; Cowley, 1975). Then we examine the amplitude of superlattice reflections as a function of crystal thickness for the superstructure of $D0_{23}$ or Al_3Zr type (space group $I4/mmm$) of Au_3X alloys (X = Mg, Zn and Cd). Finally we discuss the contrast of superstructure images in terms of the amplitude–phase diagram of superlattice reflections.

0567-7394/82/030310-08$01.00